Journal of the Ceramic Society of Japan 132 [7] 427-433 2024
DOI https://doi.org/10.2109/jcersj2.24013

JCS-Japan

FULL PAPER

Synthesis of hyperordered permanently densified silica glasses by hot compression above the glass transition temperature

Shuya Sato[1,2], Masashi Miyakawa[3], Takashi Taniguchi[3], Yohei Onodera[2], Koji Ohara[4], Kazutaka Ikeda[5], Naoto Kitamura[6], Yasushi Idemoto[6] and Shinji Kohara[2,1,†]

[1] Graduate School of Science and Technology, Tokyo University of Science, 2641 Yamazaki, Noda, Chiba 278–8510, Japan
[2] Center for Basic Research on Materials, National Institute for Materials Science, 1–2–1 Sengen, Tsukuba, Ibaraki 305–0047, Japan
[3] Research Center for Materials Nanoarchitectonics, National Institute for Materials Science, 1–1 Namiki, Tsukuba, Ibaraki 305–0044, Japan
[4] Faculty of Materials for Energy, Shimane University, 1060 Nishikawatsu-cho, Matsue 690–8504, Japan
[5] Neutron Industrial Application Promotion Center, Comprehensive Research Organization for Science and Society (CROSS), 162–1 Shirakata, Tokai, Ibaraki 319–1106, Japan
[6] Department of Pure and Applied Chemistry, Faculty of Science and Technology, Tokyo University of Science, 2641 Yamazaki, Noda, Chiba 278–8510, Japan

Synthesizing densified glasses with structure ordering is an important issue for the development of new optical fibers with high refractive index and low dispersion. Herein, we report on our attempt to synthesize densified silica (SiO_2) glasses by hot compression at a pressure of 7.7 GPa and temperatures above 1200 °C. We succeeded for the first time in recovering densified SiO_2 glasses compressed at 7.7 GPa and 1300 °C. Samples compressed above 1300 °C were crystallized into coesite by heterogeneous nucleation. The height of the first sharp diffraction peak in high-energy X-ray and neutron diffraction data of densified SiO_2 glasses increased with increasing temperature, indicating the evolution of intermediate-range ordering. Furthermore, the density increase of hot-compressed SiO_2 glasses was estimated by analyzing reduced pair distribution functions. We found that the SiO_2 glass compressed at 7.7 GPa and 1300 °C is by far the most densified and structurally ordered (hyperorderd) glass in the world.

Key-words : Densified glass, Hot compression, Structure, X-ray diffraction, Neutron diffraction

[Received February 19, 2024; Accepted May 10, 2024; Published online June 7, 2024]

1. Introduction

The theory of glass transition[1] is one of the important topics in glass science, and unraveling the glass structure is the first step to understanding the origin of glass transition. Silica (SiO_2) is a prototypical network-forming oxide material, and the SiO_2 glass has been the most intensively studied glass from ambient to extreme conditions such as high temperatures[2),3)] and high pressures,[4)–25)] since liquid SiO_2 is a "strong liquid[26)]", which results in a glass-forming material. In particular, a permanently densified SiO_2 glass is an essential scientific target to understand "polyamorphism[27)–29)]" and the formation of a "perfect glass[30)–32)]".

The synthesis of a permanently densified glass at high temperatures and pressures was reported by Mackenzie in 1963.[33),34)] Inamura et al. reported the structure and dynamics of a cold-compressed densified glass analyzed by neutron diffraction,[11),35)] Raman spectroscopy,[11)] and neutron inelastic scattering.[35)] They confirmed that a network comprising SiO_4 tetrahedra with the corner sharing of oxygen atoms is stable up to ~20 % densification. The modification of an intermediate-range structure can be ascribed to the decrease in cavity volume associated with the modification of intermediate-range ordering. They also ascribed the modification to the suppression of low-energy dynamics on the basis of their analysis of the behavior of neutron dynamical structure factors. Their conclusion is supported by a recent study by Wakabayashi et al.[36)] using Raman spectroscopy and X-ray diffraction. For in situ measurements, Sato and Funamori[17),20)] reported the results of their X-ray diffraction measurements at pressures up to 100 GPa at room temperature (RT) and they observed the transformation from SiO_4 tetrahedra to SiO_6 octahedra at 35–40 GPa. Zeidler et al. pointed out the role of SiO_5 polyhedra in tetrahedral-to-octahedral transformation on the basis of the results of neutron diffraction and classical molecular dynamics (MD) simulation.[21)] Conversely, the structural modification of SiO_2 glasses at high pressures and high temperatures is not so well understood owing to the lack of experimental information.

The most important work was conducted by Inamura et al. at high pressures up to 9.9 GPa, in which the modi-

† Corresponding author: S. Kohara; E-mail: KOHARA.Shinji@nims.go.jp

fication of the first sharp diffraction peak (FSDP) by increasing temperature up to 800 °C was observed.[16] They predicted the formation of a stable structure at high pressures, but they were unable to recover the glass under ambient conditions for consistency. Trachenko and Dove performed classical MD simulation under high pressures and high temperatures and observed rebonding during densification.[12] They also found an analog of the "reversibility window" observed in chalcogenide glasses.[13] Huang and Kieffer studied amorphous–amorphous transitions by classical MD simulation and discussed thermomechanical anomalies[14] and the densification limit.[15] However, the modification of the FSDP induced by a high temperature and a high pressure, and the amorphous–amorphous transition are still unsolved issues.

Guerette et al. reported the fabrication of densified glasses at 1100 °C and up to 8 GPa.[37] The density of the glasses they densified at 1100 °C and 8 GPa is ~25 % larger than that of a pristine glass. Furthermore, a Young's modulus increase of ~71 % relative to that of the pristine glass under ambient condition was achieved. Although they carried out X-ray diffraction measurements and MD simulation, structural differences between hot- and cold-compressed glasses are still unclear. Accordingly, it is important to clarify the structure of SiO_2 glasses synthesized above the glass transition temperature T_g of ~1180 °C to develop methods of synthesizing perfect glasses.[30)–32)] Previous studies on densified SiO_2 glasses have been reviewed in detail by Kapoor et al.[38]

Onodera et al. have recently reported the structure and density of SiO_2 glasses recovered after hot compression at a pressure of 7.7 GPa and temperatures up to 1200 °C.[39] They observed FSDP evolution in the X-ray diffraction data of glasses compressed at 7.7 GPa and a temperature higher than 400 °C. The sharpest FSDP was observed in the X-ray diffraction data of glasses compressed at 1200 °C and 7.7 GPa. They also prepared a densified glass by cold compression at a pressure of 20 GPa and RT. Although the densities of those two glasses are the same (hot-compressed glass, 2.72 g/cm^3; cold-compressed glass, 2.71 g/cm^3), FSDP evolution is only observed in the X-ray diffraction data of the hot-compressed glass. In addition, the hot-compressed glass was stable for at least 1.5 years under ambient conditions, whereas the cold-compressed glass showed a reduction in density by 2.8 % after 1.5 years, suggesting that a permanently densified SiO_2 glass can be obtained only by hot compression.

In this article, we report on the synthesis of densified SiO_2 glasses by hot compression at a pressure of 7.7 GPa and temperatures above 1200 °C because samples compressed at 7.7 GPa and above 1200 °C were found to crystallize by heterogeneous nucleation in a previous study.[39] The structure of densified SiO_2 glasses was probed by high-energy X-ray diffraction and neutron diffraction measurements in conjunction with density analysis employing the reduced pair distribution function.

2. Experiments

Densified glasses were prepared from cylindrical (5.0 mm diameter, 1.8 mm thick) synthetic fused SiO_2 (ES, Tosoh Corp.). The prepared glass sample were designated according to their processing conditions, e.g., 1300 °C/7.7 GPa refers to the glass sample recovered after hot compression at 1300 °C and 7.7 GPa. The glasses were synthesized at a pressure of 7.7 GPa and temperatures up to 1500 °C using a belt-type high-pressure apparatus (FB30H, NIMS)[40] which can generate pressures up to about 8 GPa. Since the applied pressure value was confirmed by the phase transition of Bi at 7.7 GPa, the pressure at synthesis was set to 7.7 GPa. A schematic of the apparatus is shown in **Fig. 1**(A). Because the apparatus compresses a sample through its upper and lower anvils, it has excellent

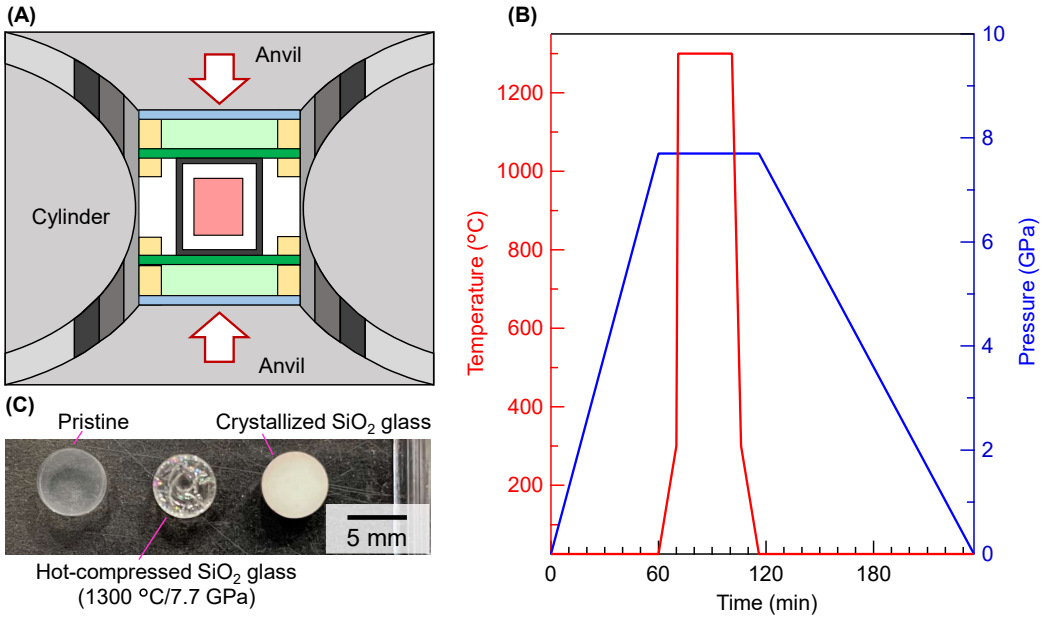

Fig. 1. Synthesis of densified SiO_2 glass. (A) Configuration of belt-type high-pressure apparatus. (B) Synthesis conditions. (C) Synthesized samples.

hydrostatic pressure and can retrieve relatively large samples for a high-pressure generator. To remove surface impurities that cause heterogeneous nucleation, the starting glass was soaked in hydrofluoric acid and hydrochloric acid for 10 min each, dried, and then sonicated with acetone for 10 min to clean its surface. The cleaned glass was encapsulated in a copper sleeve, tantalum foil, and graphite lid. The copper sleeve and tantalum foil, which forms the interface with the glass, are surface-treated by the same process as the starting glass. The synthesis conditions are shown in Fig. 1(B). The glass was compressed at a pressure of 7.7 GPa and then heated from 25 to 300 °C within 10 min and from 300 °C to target temperatures of 400, 1200, 1300, 1400, and 1500 °C within ~1 min. The target temperature was maintained for 30 min before the sample was cooled to 300 °C within 5 min and from 300 °C to RT within 10 min. Finally, the pressure was slowly released and the sample was recovered. The picture of the pristine glass, the glass densified at 1300 °C and 7.7 GPa, and the crystallized sample is shown in Fig. 1(C). It can be seen that the densified glass shows internal cracks whereas the pristine glass is transparent.

High-energy X-ray diffraction experiments were carried out on the BL04B2[41] beamline at SPring-8 (Hyogo, Japan) using the diffractometer dedicated to disordered materials. The incident X-ray energy was 61.24 keV. The diffraction patterns of glasses were measured in transmission geometry. The intensity of incident X-rays was monitored in an Ar-filled ionization chamber, and the scattered X-rays were detected by four CdTe detectors and three Ge detectors. A vacuum chamber was used to suppress air scattering around a sample. The raw data obtained were corrected for polarization, absorption, and background signals, and the contribution of Compton scattering was subtracted using a standard data analysis program.[42] Neutron diffraction measurements were conducted using on a NOVA diffractometer[43] installed on the BL21 beamline of the Materials and Life Science Facility (MLF) at the J-PARC spallation neutron source (Ibaraki, Japan). The wavelength range of the incident neutrons was $0.12\,\text{Å} < \lambda < 8.3\,\text{Å}$. The glass sample was transferred into a V–Ni null alloy cell with an outer diameter of 6.0 mm and a thickness of 0.1 mm. Each sample held in a V–Ni cell, the empty container, the empty instrument, and a vanadium standard for normalization purposes were measured. The scattering intensity observed in the sample was corrected for the background and attenuation signals of the sample and cell, and then normalized by the incident beam profile. The corrected data sets were normalized to obtain the Faber–Ziman[44] total structure factor $S(Q)$. The reduced pair distribution function $G(r)$ was obtained by a Fourier transform of $S(Q)$,

$$G(r) = \frac{2}{\pi}\int_{Q_{\min}}^{Q_{\max}} Q[S(Q) - 1]\sin(Qr)dQ. \quad (1)$$

3. Results and discussion

Figure 2(A) shows the X-ray and neutron total structure factors, $S(Q)$ of the pristine glass and a series of hot-compressed SiO_2 glasses compressed at 7.7 GPa and different temperatures. Note that the X-ray $S(Q)$ are displaced upward by 1.5 for clarity. We can see the typical structure with three peaks in neutron diffraction data: Q_1 (FSDP), Q_2 [principal peak (PP)], and Q_3. The FSDP is an important peak for discussing the formation of intermediate ordering[45)–48)] in SiO_2 glass, which reflects the periodicity of boundaries between successive cages in the network formed by connected regular SiO_4 tetrahedra with shared oxygen atoms at the corners associated with the formation of a ring structure and a cavity. The most striking feature of the $S(Q)$ of hot-compressed glasses is that the height of the FSDP in the X-ray and neutron $S(Q)$ decreases at 400 °C and increases at a temperature higher than 400 °C. The height of the FSDP reaches a maximum at 1300 °C in the X-ray $S(Q)$, whereas that of the neutron $S(Q)$ does not change so significant, suggesting that the difference arises from the different weighting factors of each atomic correlation (Si–Si, Si–O, and O–O) for X-rays and neutrons. The second peak, PP, can be observed in only neutron diffraction data, which becomes sharp with increasing temperature (density) at 7.7 GPa. This feature is consistent with that in in situ high-pressure neutron diffraction data measured at RT reported by Zeidler et al.,[21] indicating that the PP reflects the increased packing fraction of oxygen

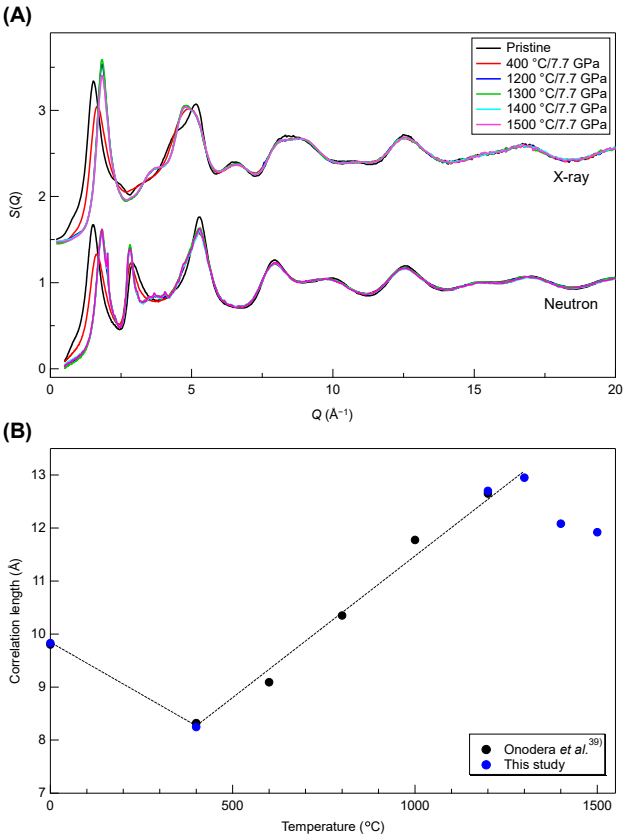

Fig. 2. (A) The X-ray and neutron total structure factors, $S(Q)$ of the pristine glass and hot-compressed SiO_2 glasses. X-ray $S(Q)$ are displaced upward by 1.5 for clarity. (B) Correlation length $2\pi/\Delta Q_{\text{FSDP}}$ extracted from the X-ray total structure factors, $S(Q)$ of the pristine glass and hot-compressed SiO_2 glasses.

atoms[49] occupying the corner of SiO_4 tetrahedra. Neutron diffraction data of the samples synthesized at temperatures above 1400 °C show a Bragg peak at approximately $Q = 2$ Å^{-1}, whereas X-ray diffraction data do not show any Bragg peaks. This is considered to be due to small amounts of crystals formed in the samples. Since the beam size in high-energy X-ray diffraction experiments is smaller than that in neutron diffraction experiments, the diffraction data from only a glassy part was observed in the X-ray diffraction measurements.

The correlation length represented by $2\pi/\Delta Q_{FSDP}$, where ΔQ_{FSDP} is the full width at half-maximum of the FSDP, was extracted from the X-ray $S(Q)$ of the pristine glass and a series of hot-compressed SiO_2 glasses using a Lorenzian function [Fig. 2(B)]. The correlation length for densified SiO_2 glasses decreases at 400 °C and then increases with processing temperature, reaching a maximum for 1300 °C/7.7 GPa, which is consistent with the behavior of the height of the FSDP. The correlation lengths for 400 °C/7.7 GPa and 1200 °C/7.7 GPa show good agreement with those reported by Onodera et al.[39] This behavior is in consistent line with that of the peak position observed at $E \sim 10$ eV of reflectance spectra in the vacuum ultraviolet region reported by Masuno et al.,[50] although the refractive index monotonically increases in hot-compressed glasses. Furthermore, a correlation length of 13.0 Å was obtained for 1300 °C/7.7 GPa, which is larger than that for 1200 °C/7.7 GPa reported by Onodera et al.,[39] demonstrating that the densified SiO_2 glass synthesized at 1300 °C/7.7 GPa is by far the most structurally ordered (hyperordered) glass in the world. Conversely, it is found that the correlation length decreases above 1400 °C. There are two possible reasons for this. The first is the possibility of melting. However, the melting point is approximately 2700 °C at 7.7 GPa, according to the phase diagram of the glass at high pressures and high temperatures reported by Zhang et al.,[51] which excludes melting as a reason. The second possibility is the effect of glass transition. Bianchi et al. demonstrated that the glass transition temperature of polyvinyl chloride tends to increase with increasing pressure.[52] Although we cannot definitively confirm that the trends for polyvinyl chloride and SiO_2 glass are the same, the glass transition temperature of SiO_2 may have increased at 7.7 GPa.

Figure 3 shows the X-ray reduced pair distribution functions $G(r)$ of the pristine glass and a series of hot-compressed SiO_2 glasses. $G(r)$ is obtained from the measured $S(Q)$ via Fourier transform, and can be described as:

$$G(r) = 4\pi r\rho[g(r) - 1], \tag{2}$$

where r is the distance in real space, ρ is the average number density of atoms, and $g(r)$ is the pair distribution function that describes the probability of finding an atomic pair separated by a certain distance r. The nearest-neighbor Si–O correlation peak is observed at approximately 1.6 Å. The $G(r)$ in the shorter distance region is given as:

$$G(r) = -4\pi r\rho. \tag{3}$$

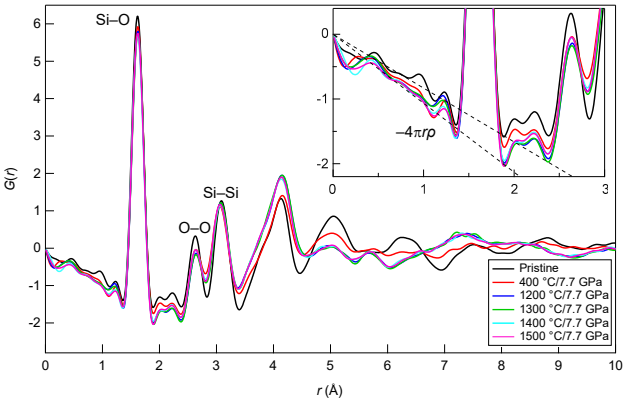

Fig. 3. The X-ray reduced pair distribution functions, $G(r)$ of the pristine glass and hot-compressed SiO_2 glasses.

Table 1. Densities of the pristine glass and hot-compressed SiO_2 glasses

	Pycnometry	Density (g/cm^3)	
		Neutron $G(r)$	X-ray $G(r)$
Pristine	2.20	2.17	2.20
400 °C/7.7 GPa	2.54[39]	2.48	2.45
1200 °C/7.7 GPa	2.72[39]	2.74	2.76
1300 °C/7.7 GPa	—	2.79	2.82
1100 °C/8.0 GPa	2.74[37]	—	—

The average number density of atoms ρ can be calculated by fitting the slope of $G(r)$ in the shorter distance region using $-4\pi r\rho$.[53),54] The obtained average number density of each sample was converted to the density d as:

$$d = \frac{\rho M_{SiO_2}}{N_A}, \tag{4}$$

where M_{SiO2} is the molar weight of SiO_2 and N_A is the Avogadro constant. The $-4\pi r\rho$ values obtained by fitting the slope of $G(r)$ of the pristine and 1300 °C/7.7 GPa samples are shown in the inset of Fig. 3. By comparing the slopes of the pristine glass and 1300 °C/7.7 GPa, we can see that the slope is steeper for the hot-compressed glass, indicating that the glasses are densified by hot compression. This behavior is also consistent with the shift of the position of the FSDP of $S(Q)$. The densities obtained by pycnometry and neutron/X-ray $G(r)$ fitting are shown in **Table 1**. Since the samples synthesized at temperatures above 1400 °C show a Bragg peak, as shown in Fig. 2(A), the calculated density may be estimated to be higher owing to the locally crystallized area. Therefore, the density was calculated for the samples synthesized below 1300 °C. The discrepancy between the densities obtained by pycnometry and $G(r)$ fitting for the pristine, 400 °C/7.7 GPa, and 1200 °C/7.7 GPa samples are within 5 %.

Figure 4 shows the densities of the glasses synthesized at 7.7 GPa and different temperatures together with those of a series of crystalline phases. The density of the glass compressed at 7.7 GPa rapidly increases up to 600 °C and then gradually increases with further increase in processing temperature. This behavior is completely different

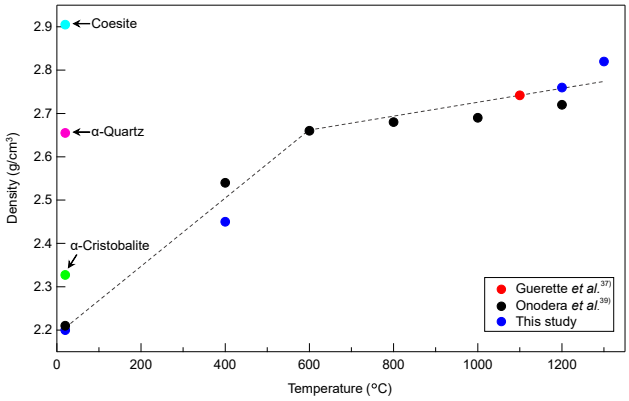

Fig. 4. Density of the glasses synthesized at 7.7 GPa and different temperatures.

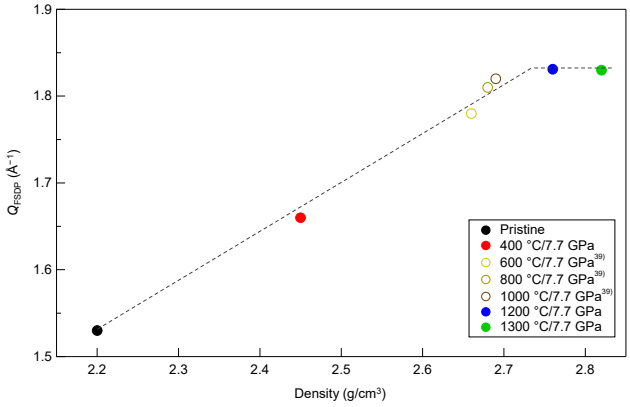

Fig. 5. The density dependence of the position of FSDP for the pristine glass and hot-compressed SiO_2 glasses.

from that in cold-compressed glasses reported by Sato and Funamori, in which the density changed monotonically with increasing pressure.[18] The density of the 1300 °C/7.7 GPa sample of approximately 2.8 g/cm^3 is higher than that of the 1100 °C/8 GPa glass synthesized by Guerette et al. (2.74 g/cm^3).[37] Thus, the densified SiO_2 glass obtained at 1300 °C/7.7 GPa could be considered the most densified SiO_2 glass, which should have the highest refractive index.[51] Note that glass crystallizes into coesite when the temperature is greater than 1200 °C/7.7 GPa, as shown in our previous study.[39]

Figure 5 shows the density dependence of the position of the FSDP in the X-ray $S(Q)$. The position of the FSDP shifts with increasing temperature (density) up to 1200 °C and does not shift above 1300 °C. Onodera et al. reported that the cavity volume ratio of the SiO_2 glass synthesized at 1200 °C/7.7 GPa was reduced to 6 %,[39] as determined by the cavity volume analysis of the MD-RMC model. This behavior indicates that a marked reduction in cavity volume is induced by the hot compression of SiO_2 glass. The nonshifting of the FSDP may be due to the reduction in cavity volume.

Figures 6(A) and 6(B) show the X-ray and neutron total correlation functions, $T(r)$ of the pristine glass and a series of hot-compressed SiO_2 glasses synthesized up to 1300 °C/

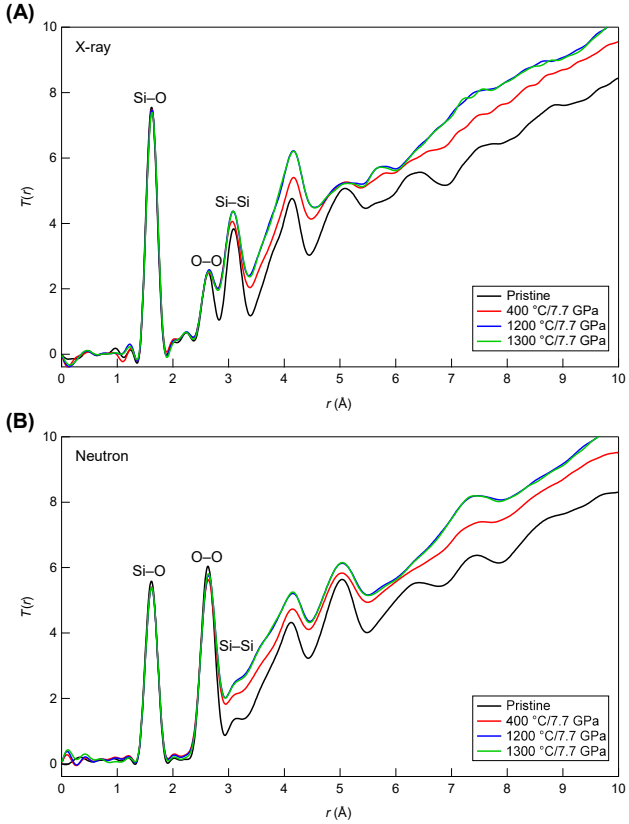

Fig. 6. Total correlation functions, $T(r)$ of the pristine glass and hot-compressed SiO_2 glasses obtained from (A) X-ray and (B) neutron diffraction.

Table 2. Si–O coordination numbers of the pristine glass and hot-compressed SiO_2 glasses

	Neutron $T(r)$	X-ray $T(r)$
Pristine	4.0	4.0
400 °C/7.7 GPa	4.0	3.9
1200 °C/7.7 GPa	4.0	3.9
1300 °C/7.7 GPa	4.0	3.9

7.7 GPa. The peaks observed at 1.61, 2.65, and 3.08 Å can be ascribed to Si–O, O–O, and Si–Si correlations, respectively. As can be seen in the figure, the contrast between the X-ray and neutron diffraction data is excellent. The O–O correlation peak is prominent in neutron diffraction data since neutrons are sensitive to oxygen atoms, whereas the Si–Si correlation peak is clearly detected in X-ray data since X-rays are sensitive to heavy elements. The area of the Si–O correlation peak was almost the same for all samples. Since this area reflects the coordination number of O atoms around a Si atom, the same area means that the coordination number of all samples is identical. Since the Si–O coordination number in SiO_2 glass is four, the area of the peak in all samples was calculated by curve fitting and comparing it with the peak area of the sample before compression.[55] The Si–O coordination numbers derived from the experimental $T(r)$ are shown in **Table 2**. The Si–O coordination number of four was obtained in all glasses, indicating that a SiO_4 tetrahedral network is stable in a

series of densified glasses, which agrees well with other densified glasses.[11),37)] In contrast, the O–O and Si–Si correlation peaks become broad with increasing density.

4. Conclusions

We investigated the densified SiO_2 glasses synthesized by hot compression. Although local crystallization has been observed at temperatures above 1300 °C at 7.7 GPa, we succeeded in synthesizing the glasses without crystallization up to temperatures of 1300 °C/7.7 GPa and found that SiO_2 glass synthesized at 1300 °C/7.7 GPa is by far the most structurally ordered (hyperordered) SiO_2 glass in the world on the basis of the analysis of the FSDP of the structure factor $S(Q)$ obtained from X-ray and neutron diffraction measurements. The structural ordering decreases at temperatures above 1400 °C/7.7 GPa, which may be due to glass transition. The density obtained from the reduced pair distribution function $G(r)$ suggests that the density of the SiO_2 glass synthesized at 1300 °C/7.7 GPa is higher than 2.75 g/cm^3, which is the highest density among the samples synthesized thus far. At 7.7 GPa, the synthesis temperature of the SiO_2 glass with the highest density and structural ordering was 1300 °C. The effects of these structures on mechanical and optical properties[56)] and relationship with synthesis conditions will be investigated as a next step.

Acknowledgements This work was supported by JST SPRING, Grant Number JPMJSP2151 (to S.S.), Grant-in-Aid for Transformative Research Areas (A) Hyper-Ordered Structure, Grant Numbers 20H05878 (to S.K.), 20H05880 (to N.K.), and 20H05881 (to Y.O. and S.K.), for Scientific Research on Innovative Areas, Grant Number 19H05790 (to M.M.) and World Premier International Research Center Initiative (WPI), MEXT, Japan.

The X-ray diffraction measurements were conducted at SPring-8 with the approval of Japan Synchrotron Radiation Research Institute (JASRI) (Proposal No.: 2022A1002). The neutron diffraction experiments at the MLF of the J-PARC were performed under a long-term proposal (Proposal No. 2022L0202). Discussions with Profs. M. Ono and A. Masuno, and Drs. H. Yusa, H. Masai, H. Segawa, and Y. Shuseki are gratefully appreciated. We thank M. Kawasaki for processing the glass.

References

1) J. S. Langer, *Rep. Prog. Phys.*, 77, 042501 (2014).
2) A. Takada, P. Richet, C. R. A. Catlow and G. D. Price, *J. Non-Cryst. Solids*, 345–346, 224–229 (2004).
3) Q. Mei, C. J. Benmore and J. K. R. Weber, *Phys. Rev. Lett.*, 98, 057802 (2007).
4) P. McMillan, B. Piriou and R. Couty, *J. Chem. Phys.*, 81, 4234–4236 (1984).
5) M. Grimsditch, *Phys. Rev. Lett.*, 52, 2379–2381 (1984).
6) R. J. Hemley, H. K. Mao, P. M. Bell and B. O. Mysen, *Phys. Rev. Lett.*, 57, 747–750 (1986).
7) S. Susman, K. J. Volin, D. L. Price, M. Grimsditch, J. P. Rino, R. K. Kalia, P. Vashishta, G. Gwanmesia, Y. Wang and R. C. Liebermann, *Phys. Rev. B*, 43, 1194–1197 (1991).
8) C. Meade, R. J. Hemley and H. K. Mao, *Phys. Rev. Lett.*, 69, 1387–1390 (1992).
9) S. Sugai, H. Sotokawa, D. Kyokane and A. Onodera, *Physica B*, 219–220, 293–295 (1996).
10) S. Sugai and A. Onodera, *Phys. Rev. Lett.*, 77, 4210–4213 (1996).
11) Y. Inamura, M. Arai, N. Kitamura, S. M. Bennington and A. C. Hannon, *Physica B*, 241–243, 903–905 (1998).
12) K. Trachenko and M. Dove, *Phys. Rev. B*, 67, 064107 (2003).
13) K. Trachenko and M. Dove, *Phys. Rev. B*, 67, 212203 (2003).
14) L. Huang and J. Kieffer, *Phys. Rev. B*, 69, 224203 (2004).
15) L. Huang and J. Kieffer, *Phys. Rev. B*, 69, 224204 (2004).
16) Y. Inamura, Y. Katayama, W. Utsumi and K. Funakoshi, *Phys. Rev. Lett.*, 93, 015501 (2004).
17) T. Sato and N. Funamori, *Rev. Sci. Instrum.*, 79, 073906 (2008).
18) T. Sato and N. Funamori, *Phys. Rev. Lett.*, 101, 255502 (2008).
19) C. J. Benmore, E. Soignard, S. A. Amin, M. Guthrie, S. D. Shastri, P. L. Lee and J. L. Yarger, *Phys. Rev. B*, 81, 054105 (2010).
20) T. Sato and N. Funamori, *Phys. Rev. B*, 82, 184102 (2010).
21) A. Zeidler, K. Wezka, R. F. Rowlands, D. A. J. Whittaker, P. S. Salmon, A. Polidori, J. W. E. Drewitt, S. Klotz, H. E. Fischer, M. C. Wilding, C. L. Bull, M. G. Tucker and M. Wilson, *Phys. Rev. Lett.*, 113, 135501 (2014).
22) M. Murakami, S. Kohara, N. Kitamura, J. Akola, H. Inoue, A. Hirata, Y. Hiraoka, Y. Onodera, I. Obayashi, J. Kalikka, N. Hirao, T. Musso, A. S. Foster, Y. Idemoto, O. Sakata and Y. Ohishi, *Phys. Rev. B*, 99, 045153 (2019).
23) Y. Kono, Y. Shu, C. Kenney-Benson, Y. Wang and G. Shen, *Phys. Rev. Lett.*, 125, 205701 (2020).
24) A. Hasmy, S. Ispas and B. Hehlen, *Nature*, 599, 62–66 (2021).
25) Y. Kono, K. Ohara, N. M. Kondo, H. Yamada, S. Hiroi, F. Noritake, K. Nitta, O. Sekizawa, Y. Higo, Y. Tange, H. Yumoto, T. Koyama, H. Yamazaki, Y. Senba, H. Ohashi, S. Goto, I. Inoue, Y. Hayashi, K. Tamasaku, T. Osaka, J. Yamada and M. Yabashi, *Nat. Commun.*, 13, 2292 (2022).
26) C. A. Angell, *Science*, 267, 1924–1935 (1995).
27) O. Mishima and H. E. Stanley, *Nature*, 396, 329–335 (1998).
28) Y. Katayama, T. Mizutani, W. Utusmi, O. Shimomura, M. Yamakata and K. Funakoshi, *Nature*, 403, 170–173 (2000).
29) P. F. McMillan, M. Wilson, M. C. Wilding, D. Daisenberger, M. Mezouar and G. N. Greaves, *J. Phys.-Condens. Mat.*, 19, 415101 (2007).
30) C. A. Angell, C. T. Moynihan and M. Hemmati, *J. Non-Cryst. Solids*, 274, 319–331 (2000).
31) G. N. Greaves and S. Sen, *Adv. Phys.*, 56, 1–166 (2007).
32) L. Wondraczek, G. Gao, D. Möncke, T. Selvam, A. Kuhnt, W. Schwieger, D. Palles and E. I. Kamitsos,

J. Non-Cryst. Solids, 360, 36–40 (2013).
33) J. D. Mackenzie, *J. Am. Ceram. Soc.*, 46, 461–470 (1963).
34) J. D. Mackenzie, *J. Am. Ceram. Soc.*, 46, 470–476 (1963).
35) Y. Inamura, M. Arai, M. Nakamura, T. Otomo, N. Kitamura, S. M. Bennington, A. C. Hannon and U. Buchenau, *J. Non-Cryst. Solids*, 293–295, 389–393 (2001).
36) D. Wakabayashi, N. Funamori, T. Sato and T. Taniguchi, *Phys. Rev. B*, 84, 144103 (2011).
37) M. Guerette, M. R. Ackerson, J. Thomas, F. Yuan, E. B. Watson, D. Walker and L. Huang, *Sci. Rep.-UK*, 5, 15343 (2015).
38) S. Kapoor, L. Wondraczek and M. M. Smedskjaer, *Front. Mater.*, 4, 1–20 (2017).
39) Y. Onodera, S. Kohara, P. S. Salmon, A. Hirata, N. Nishiyama, S. Kitani, A. Zeidler, M. Shiga, A. Masuno, H. Inoue, S. Tahara, A. Polidori, H. E. Fischer, T. Mori, S. Kojima, H. Kawaji, A. I. Kolesnikov, M. B. Stone, M. G. Tucker, M. T. McDonnell, A. C. Hannon, Y. Hiraoka, I. Obayashi, T. Nakamura, J. Akola, Y. Fujii, K. Ohara, Y. Taniguchi and O. Sakata, *NPG Asia Mater.*, 12, 85 (2020).
40) S. Yamaoka, M. Akashi, H. Kanda, T. Osawa, T. Taniguchi, H. Sei and O. Fukunaga, *J. High Pressure Inst. Jpn.*, 30, 249–258 (1992).
41) K. Ohara, Y. Onodera, M. Murakami and S. Kohara, *J. Phys.-Condens. Mat.*, 33, 383001 (2021).
42) S. Kohara, M. Itou, K. Suzuya, Y. Inamura, Y. Sakurai, Y. Ohishi and M. Takata, *J. Phys.-Condens. Mat.*, 19, 506101 (2007).
43) T. Otomo, K. Suzuya, M. Misawa, N. Kaneko, H. Ohshita, K. Ikeda, M. Tsubota, T. Seya, T. Fukunaga, K. Itoh, M. Sugiyama, K. Mori, Y. Kameda, T. Yamaguchi, K. Yoshida, K. Maruyama, Y. Kawakita, S. Shamoto, K. Kodama, S. Takata, S. Satoh, S. Muto, T. Ino, H. M. Shimizu, T. Kamiyama, S. Ikeda, S. Itoh, Y. Yasu, K. Nakayoshi, H. Sendai, S. Uno, M. Tanaka and K. Ueno, *KENS Rep.*, 17, 28–36 (2011).
44) T. E. Faber and J. M. Ziman, *Philos. Mag.*, 11, 153–173 (1965).
45) D. L. Price, S. C. Moss, R. Reijers, M. L. Saboungi and S. Susman, *J. Phys. C Solid State*, 21, L1069–L1072 (1988).
46) S. R. Elliott, *Nature*, 354, 445–452 (1991).
47) P. S. Salmon, R. A. Martin, P. E. Mason and G. J. Cuello, *Nature*, 435, 75–78 (2005).
48) Y. Onodera, S. Kohara, S. Tahara, A. Masuno, H. Inoue, M. Shiga, A. Hirata, K. Tsuchiya, Y. Hiraoka, I. Obayashi, K. Ohara, A. Mizuno and O. Sakata, *J. Ceram. Soc. Jpn.*, 127, 853–863 (2019).
49) A. Zeidler, P. S. Salmon and K. B. Skinner, *P. Natl. Acad. Sci. USA*, 111, 10045–10048 (2014).
50) A. Masuno, N. Nishiyama, F. Sato, N. Kitamura, T. Taniguchi and H. Inoue, *RSC Adv.*, 6, 19144–19149 (2016).
51) J. Zhang, B. Li, W. Utsumi and R. C. Liebermann, *Phys. Chem. Miner.*, 23, 1–10 (1996).
52) U. Bianchi, A. Turturro and G. Basile, *J. Phys. Chem.-US*, 71, 3555–3558 (1967).
53) R. Kaplow, S. L. Strong and B. L. Averbach, *Phys. Rev.*, 138, A1336–A1345 (1965).
54) G. S. E. Antipas and K. T. Karalis, *MethodsX*, 6, 601–605 (2019).
55) K. Sugiyama, E. Matsubara, I. K. Sue, Y. Waseda and J. M. Toguri, *Sci. Rep. Res. Tohoku A*, 34A, 143–154 (1989).
56) K. A. Kirchner, D. R. Cassar, E. D. Zanotto, M. Ono, S. H. Kim, K. Doss, M. L. Bødker, M. M. Smedskjaer, S. Kohara, L. Tang, M. Bauchy, C. J. Wilkinson, Y. Yang, R. S. Welch, M. Mancini and J. C. Mauro, *Chem. Rev.*, 123, 1774–1840 (2023).